

Award Number: 08HQGR0084

Depth of Faulting in Large Strike-Slip Earthquakes

Final Report

November 30, 2009

Seok Goo Song and Paul Somerville
(Contact Email: Seok_Goo_Song@URSCorp.com)

URS Group, Inc.
566 El Dorado Street
Pasadena, CA 91101-2560
Tel: (626) 449-7650
Fax: (626) 449-3536

Abstract

This report addresses the depth of coseismic faulting and its implications for seismic hazard analysis and the prediction of strong ground motion. In rupture model inversions, the largest slip typically occurs at depths between 5 and 10 km, and is tapered both above and below that depth range. This depth distribution of slip is attributable to changes in frictional behavior with depth. It is thought that earthquakes can only initiate by slip weakening in a zone of limited depth range where dynamic friction is less than static friction. However, once rupture begins, it can propagate into stable regions. Consequently, small earthquakes rarely break the surface, and their slip is limited to seismogenic depths. In contrast, large earthquakes propagate upward from the seismogenic zone to the surface, and also propagate downward below the seismogenic zone. This model appears to be inconsistent with the assumption, used by the Working Group for California Earthquake Probabilities (WGCEP), that the base of the coseismic zone is defined by the base of background seismicity, because slip inverted from large earthquakes often extends below the base of background seismicity. If the WGCEP approach is indeed underestimating fault rupture width in past earthquakes based on background seismicity, this has significant implications for characterizing earthquake rupture models for the prediction of strong ground motions. For example, it would lead to underestimation of rupture area and hence overestimation of fault slip (typically a factor of 2) for a given seismic moment. Simulations of strong ground motions using such relationships between seismic moment and rupture area produce ground motions that are much larger than recorded ground motions. Also, the assumption of narrow fault rupture widths in past earthquakes leads to magnitude – area scaling relations compatible with the L model, in which fault slip grows linearly with fault length for earthquakes whose rupture widths have saturated. The L model implies that ground motion scaling with magnitude should increase above about M 6.7, but empirical ground motion models show the opposite trend, with ground motion scaling decreasing for larger magnitudes. In this report, we perform detailed studies of the depth resolution of coseismic slip estimate for a real strike-slip event, e.g., 1999 Kocaeli, Turkey, earthquake, by inverting both geodetic and seismic data. We found that deep slip below the seismogenic zone cannot be resolved by the geodetic data alone, although it exists, and joint inversion of both geodetic and seismic data may improve our capability to resolve the deep slip. Non-physical regularization used in most ill-posed earthquake source inversions also prevent us from resolving the deep slip accurately. In this report, we suggest a new inversion approach based on the Bayesian inversion, in which we can use physically-guided regularization instead of the nonphysical Tikhonov regularization. This project is expected to lead to reduction in the large degree of uncertainty in the rupture widths of large strike-slip earthquakes, which at present results in a large amount of unmodeled epistemic uncertainty in the characterization of the earthquake sources used in the National Seismic Hazard Maps, and hence in the ground motion values in these maps.

1. Depth of Coseismic Faulting

This report addresses the depth of coseismic faulting and its implications for seismic hazard analysis and the prediction of strong ground motion. This issue was encountered by the Working Group for California Earthquake Probabilities in the course of developing a uniform earthquake rupture forecast for California (Stein, 2006). The approach adopted by the Working Group was to assume that the base of the coseismic zone is defined by the base of background seismicity. The advantage of this approach is that it can be applied uniformly throughout a region containing many faults on which historical earthquakes have not occurred, but it may have serious shortcomings. The basis of this assumption is the analysis of Nazareth and Hauksson (2004) which compared the maximum depth of pre-mainshock background seismicity with the depth to the bottom of rupture of moderate to large earthquakes in Southern California derived from rupture model inversions (Figure 1). Nazareth and Hauksson (2004) and the Working Group (WGCEP, 2003; Ellsworth, 2006; Stein, 2006) hypothesize from this figure that the maximum depth of background

seismicity provides an unbiased estimate of the depth to the bottom of rupture in large earthquakes (which we term the coseismic depth). However, the numerous data points above the diagonal line in Figure 1 indicate that, as a general rule, the depth to the base of the coseismic zone of moderate to large earthquakes exceeds that of the background seismicity, and thus the hypothesis used by the Working Group may not be correct.

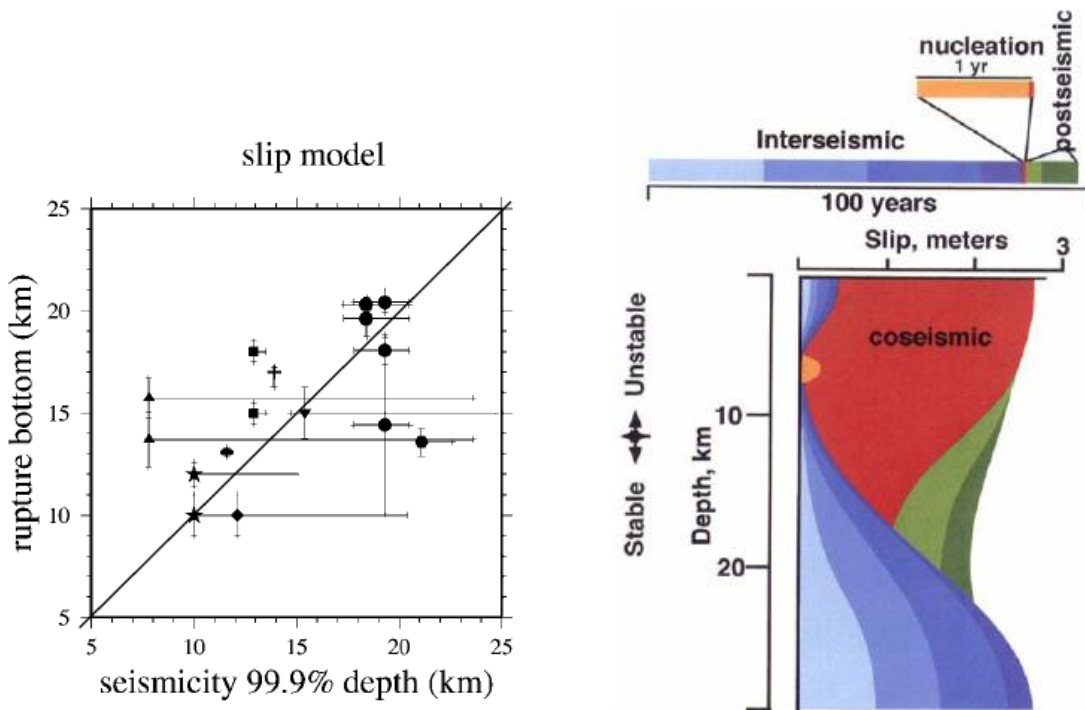


Figure 1. [left] Relation between mainshock rupture depth and the depth of background seismicity. The circles are various estimates for the 1994 Northridge earthquake. Source: Nazareth and Hauksson (2004), with diagonal line added. [right] Schematic diagram of the brittle seismogenic zone (orange) and the coseismic zone (red). Source: Scholz (2002).

As an extreme example which we discuss in more detail below, many rupture model inversions of the 2002 Denali, Alaska earthquake based on seismological data have rupture widths as large as 30 km (e.g. Oglesby et al., 2004; Thio, 2005), whereas the base of the background seismicity is at a depth of 12 km. Some 2006 WGCEP members consider that rupture model inversions do not provide reliable estimates of the depth of rupture. We conclude that there exists a large degree of epistemic uncertainty in the rupture widths of large earthquakes, and in the relationship between magnitude and fault rupture area, that is not being addressed by the WGCEP. Since it is intended that the WGCEP results be used in future revisions of the National Seismic Hazard Map, and that these maps should treat all significant sources of epistemic uncertainty, it is important that this epistemic uncertainty be investigated and reduced. The depth distribution of slip, averaged along strike, inferred from rupture model inversions of several recent large strike-slip earthquakes is shown in Figure 2. The largest slip typically occurs at depths between 5 and 10 km, and is tapered both above and below that depth range. This depth distribution of slip is attributable to changes in frictional behavior with depth. Dieterich (1972) and Scholz (1972) suggested that earthquakes can only initiate by slip weakening in a zone of limited depth range (which we term the seismogenic zone) where dynamic friction is less than static friction, indicated by the small orange zone in the right panel of

Figure 1. However, once rupture begins, it can propagate into stressed regions where static and dynamic friction are equal, indicated by the large red coseismic zone in Figure 1 (right panel). Consequently, small earthquakes ($M < 6$) rarely break the surface, and their slip is limited to seismogenic depths. In contrast, large earthquakes propagate upward from the seismogenic zone to the surface, and also propagate downward below the seismogenic zone, to occupy the coseismic zone shown in red in Figure 1 (right panel). The depth distribution of slip is expected to be controlled by depth dependent shear strength and frictional properties (Mikumo, 1992).

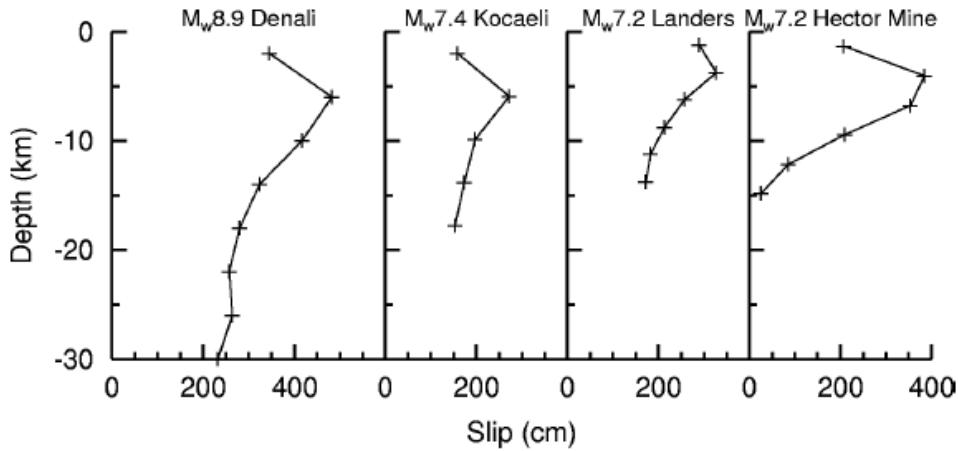


Figure 2. Distribution of slip with depth in strike-slip earthquakes, averaged along strike. Source: Somerville and Pitarka (2006).

2. Depth Resolution of Earthquake Rupture from Geodetic Data

King and Wesnousky (2007) have proposed a model, shown in Figure 3, in which fault slip is tapered in a manner like that of the earthquakes shown in Figure 2. The tapered shape represents the transition from brittle to ductile behavior that occurs both at the top and bottom of the seismogenic zone. In this model, the strain drop (ratio of average displacement to fault width) is constant, instead of increasing with earthquake magnitude as occurs in the box model that is also shown in Figure 3, but the geodetic displacements of the ground for each pair of models (tapered and box) are virtually identical, as shown for one pair on the left panel of Figure 3. This study clearly indicates that deep slip below the seismogenic zone, although they may exist, may not be detectable by geodetic data only inversion.

We performed geodetic slip inversion for a strike-slip event (the 1999 Kocaeli, Turkey, event) to test the resolving power of geodetic data, especially as a function of depth. Figure 4 shows the 7 segment fault trace (black solid lines) for the event with horizontal component static fields from Reilinger et al. (2000). We used the singular value decomposition (SVD) to invert the geodetic data and to estimate coseismic slip distribution on the fault planes with 4 km by 4 km grid spacing. With the SVD, the model estimator can be represented as given in equation (1). Both model resolution and covariance matrices can be computed as in equations (2) and (3), respectively. p is the number of singular values used in the calculation.

$$\hat{\mathbf{m}} = \mathbf{G}^\dagger \mathbf{d} = \mathbf{V}_p \mathbf{S}_p^{-1} \mathbf{U}_p^T \mathbf{d} \quad (1)$$

$$\mathbf{R}_m = \mathbf{G}^\dagger \mathbf{G} = \mathbf{V}_p \mathbf{V}_p^T \quad (2)$$

$$\mathbf{C}_m = \mathbf{G}^\dagger \mathbf{C}_d \mathbf{G}^{\dagger T} \quad (3)$$

In the generalized inversion with the SVD, the number of singular values controls the stability and resolution of the inversion. If a large number of singular values is used in the inversion, high model resolution can be achieved, but stability is reduced, and vice versa. This is the well-known trade-off between model resolution and covariance matrices in geophysical inverse problems. Figure 5 shows the sequence of singular values for the geodetic inversion of the Kocaeli event. By adjusting the number of singular values used in the inversion, we can easily illustrate the trade-off between the model resolution and covariance matrices and how much deep slip can be resolved by inverting geodetic data observed on the surface.

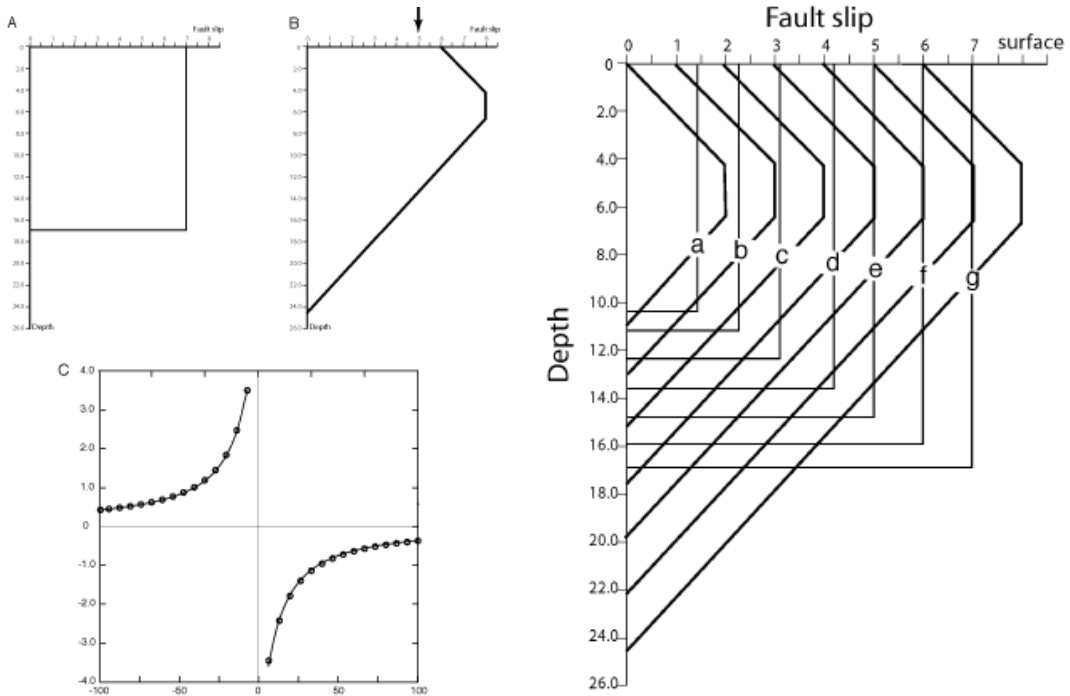


Figure 3. [left] Box and tapered models (top) of depth distribution of strike-slip earthquakes having almost identical displacement fields (bottom). Circles and lines are from the box and tapered models, respectively (King and Wesnousky, 2007). [right] Pairs of box and tapered depth profiles of slip that produce the same displacement field at the ground surface (King and Wesnousky, 2007).

We used three sets of singular values, $p = 50, 25,$ and $15,$ and computed coseismic slip and model resolution and covariance matrices for each set of singular values (Figures 6, 7, and 8). As predicted from inverse theory, a large number of singular values introduces a high level of instability in the inversion (see the top panel of Figure 8) although it may lead to relatively high resolution in the estimation. However, especially in the geodetic inversion, the resolution of the inversion decays rapidly as a function of depth

(see Figure 7). Although we increase the number of singular values (from $p = 15$ to $p = 50$), the resolution at depth is not increased significantly (see the top panel of Figure 7). If we keep a reasonable level of stability in the inversion (e.g., $p = 15$), the geodetic data for the Kocaeli event have almost no resolving power below 8 ~ 10 km (see the bottom panel of Figure 7). Thus we are not able to resolve whether the estimated slip below this depth in the bottom panel of Figure 6 is a real feature constrained by data.

Figure 4 shows the predicted static field from estimated slip distribution in the bottom panel of Figure 6 ($p = 15$). The variance reduction (VR) computed for this model with the equation given below is 96.3 % and VRs for slip estimates in the top and center panels of Figure 6 are 99.6 % and 98.9 %, respectively. This indicates that statistically speaking all three slip estimates produce about the same level of data fitting, which means that the level of data fitting does not necessarily indicate the quality of model estimates.

$$VR = \left(1 - \frac{(\mathbf{d} - \mathbf{G}\mathbf{m})^T \mathbf{C}_d^{-1} (\mathbf{d} - \mathbf{G}\mathbf{m})}{\mathbf{d}^T \mathbf{C}_d^{-1} \mathbf{d}} \right) \times 100 \% \quad (4)$$

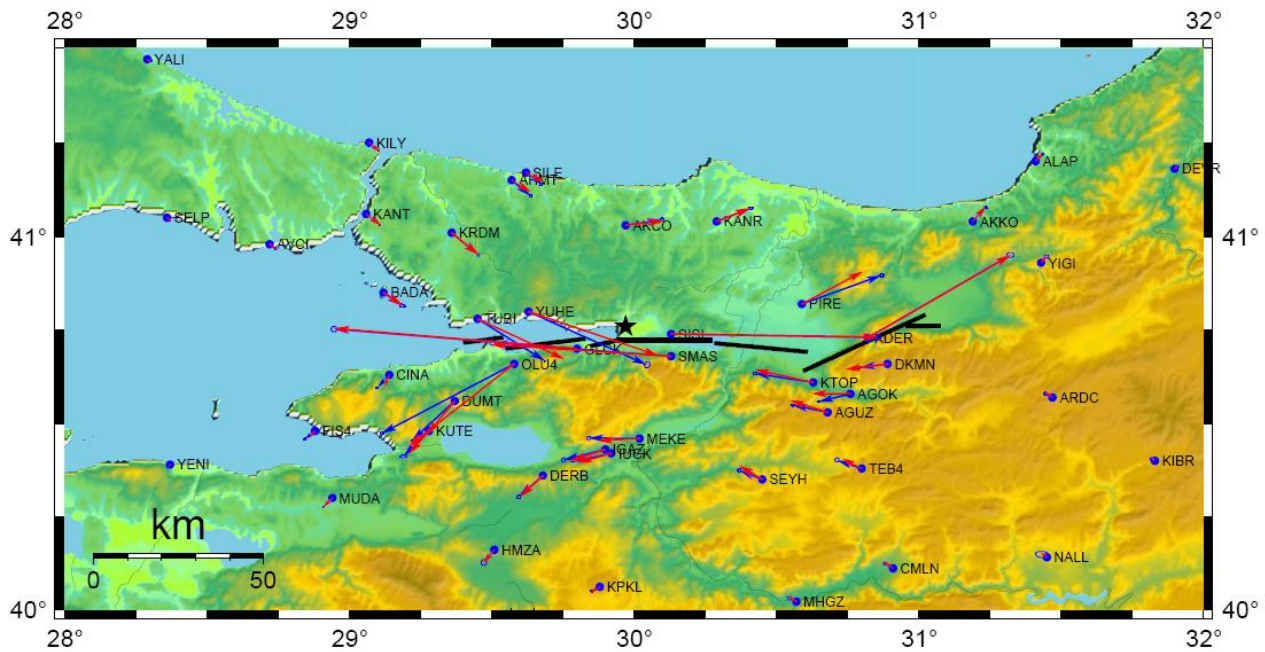


Figure 4. GPS data (blue) with synthetic predictions (red) for the 1999 Kocaeli, Turkey, event. Data source: Reilinger et al. (2000).

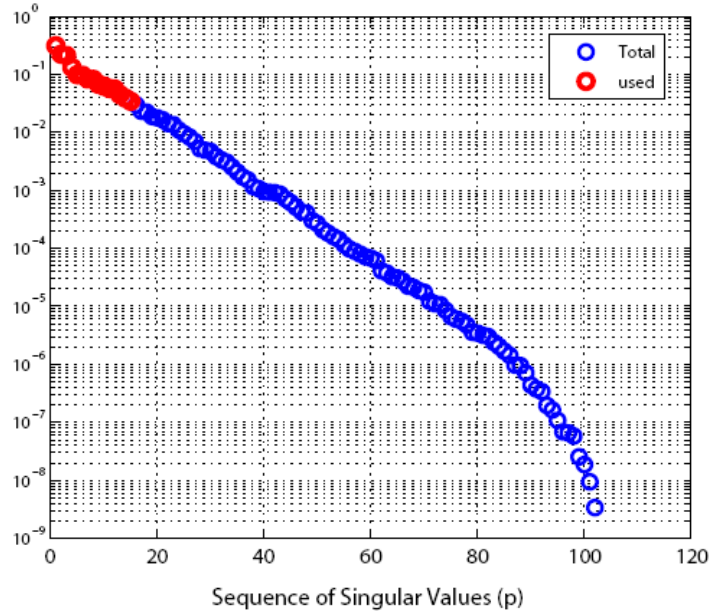


Figure 5. Sequence of total singular values (blue) for the geodetic inversion of the Kocaeli, Turkey, event, with the first 15 largest ones in red.

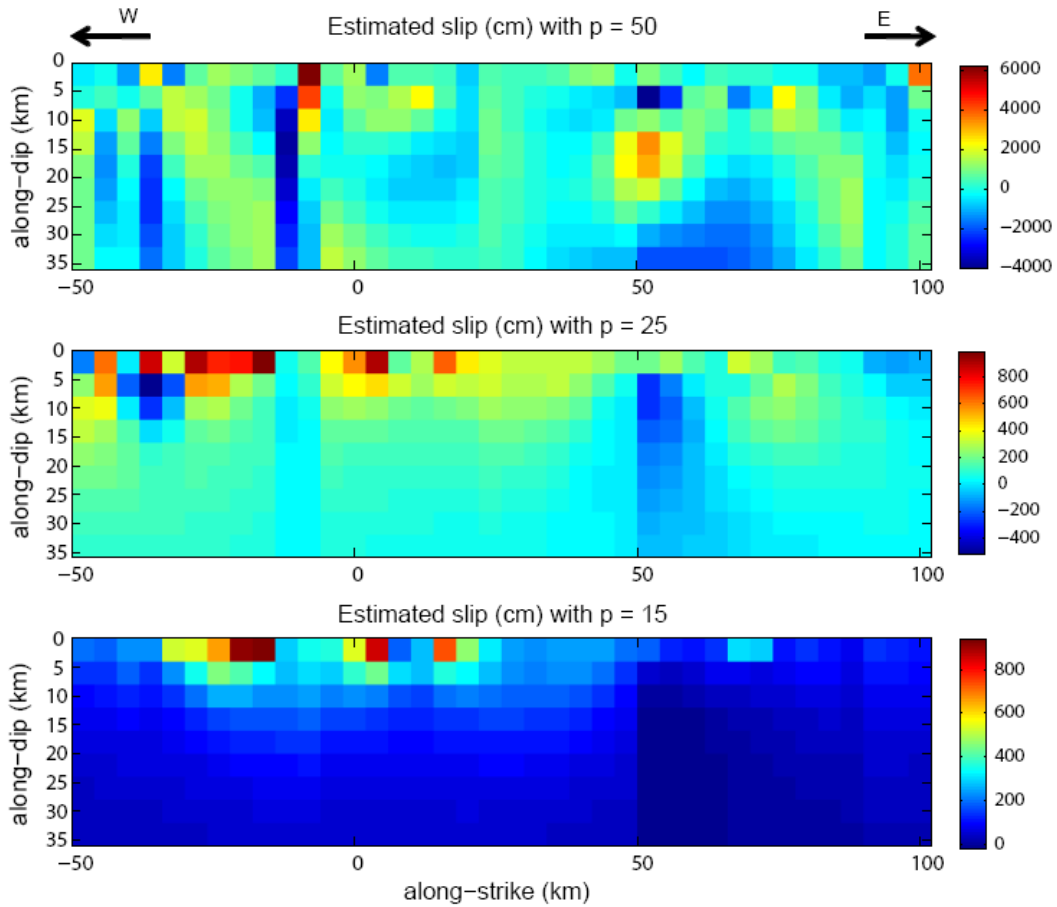


Figure 6. Estimated slip distributions by inverting GPS data with three different sets of singular values (top: $p=50$, center: $p=25$, bottom: $p=15$).

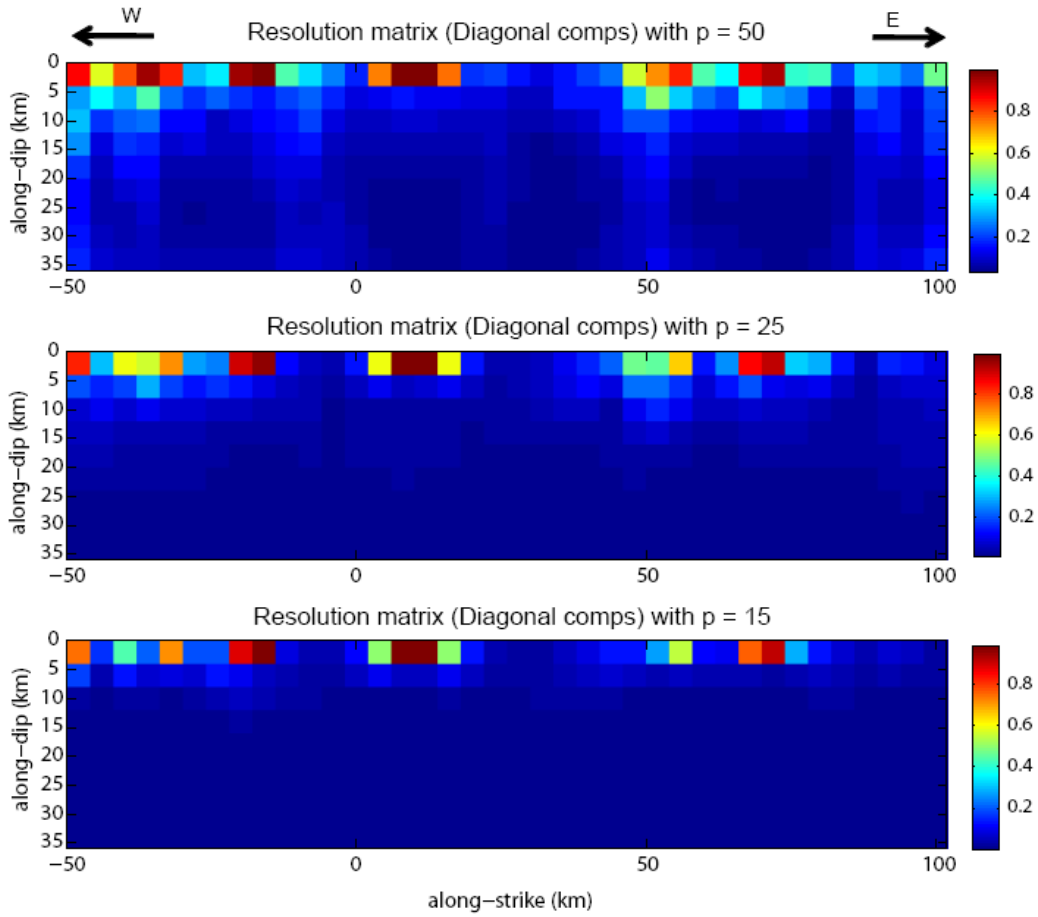


Figure 7. Diagonal components of model resolution matrix for each subfault (top: $p=50$, center: $p=25$, bottom: $p=15$).

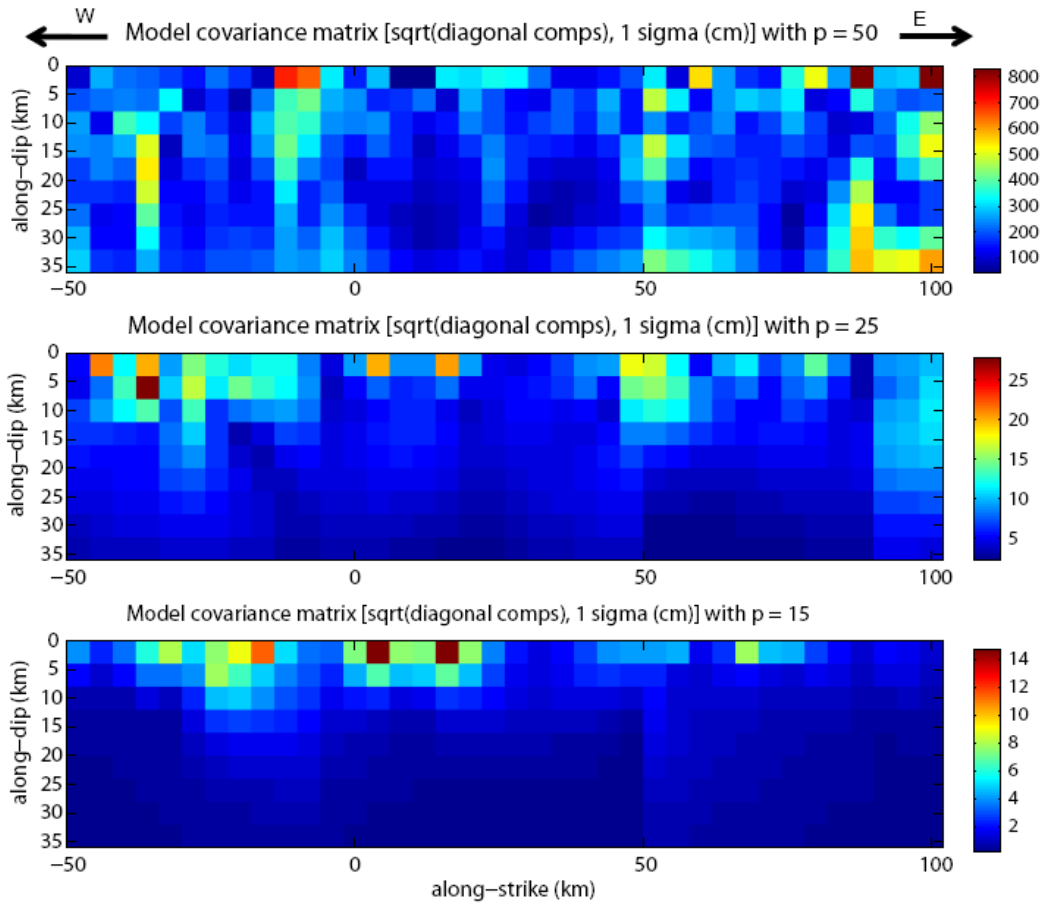


Figure 8. Standard deviation of slip estimators for each subfault (top: $p=50$, center: $p=25$, bottom: $p=15$).

3. Depth Resolution of Earthquake Rupture from Joint Inversion

As demonstrated in the section above, the static displacement field decays rapidly from the source and it is very difficult to constrain slip at depth by inverting geodetic data only. On the other hand, seismic data may deliver information about source processes at farther distances. In particular, ray paths of teleseismic data are mostly down going with small take-off angles. This makes teleseismic data relatively sensitive to the relative location of slip, particularly in the down-dip direction. In this section, we analyze model resolution for each type of inversion, e.g., geodetic, teleseismic, and combined (joint) inversion, and examine how each kind of data contributes to constrain certain elements of source processes.

Figure 9 shows the diagonal components of model resolution matrices obtained by inverting three different sets of data, e.g., GPS (top), teleseismic (center), and combined (bottom). It clearly indicates that the model resolution from the geodetic data decays rapidly as a function of depth while the model resolution from the teleseismic data is evenly distributed over the entire fault plane. It is interesting to see that the model resolution near the surface is very low in the teleseismic inversion. This is because direct P phases at teleseismic distance are cancelled out by the surface reflected P phases (pP and sP). The bottom panel of Figure 9 and Figure 10 show that we can benefit from both data sets by jointly inverting both geodetic and seismic data. Relatively high resolution is achieved near the surface from the geodetic data, but it does not decay as much as in the inversion using only geodetic data. A linearized single time

window method is used for both teleseismic and joint inversion (Thio et al., 2004) since final static slip is a main interest of this study rather than fine details of temporal evolution of slip.

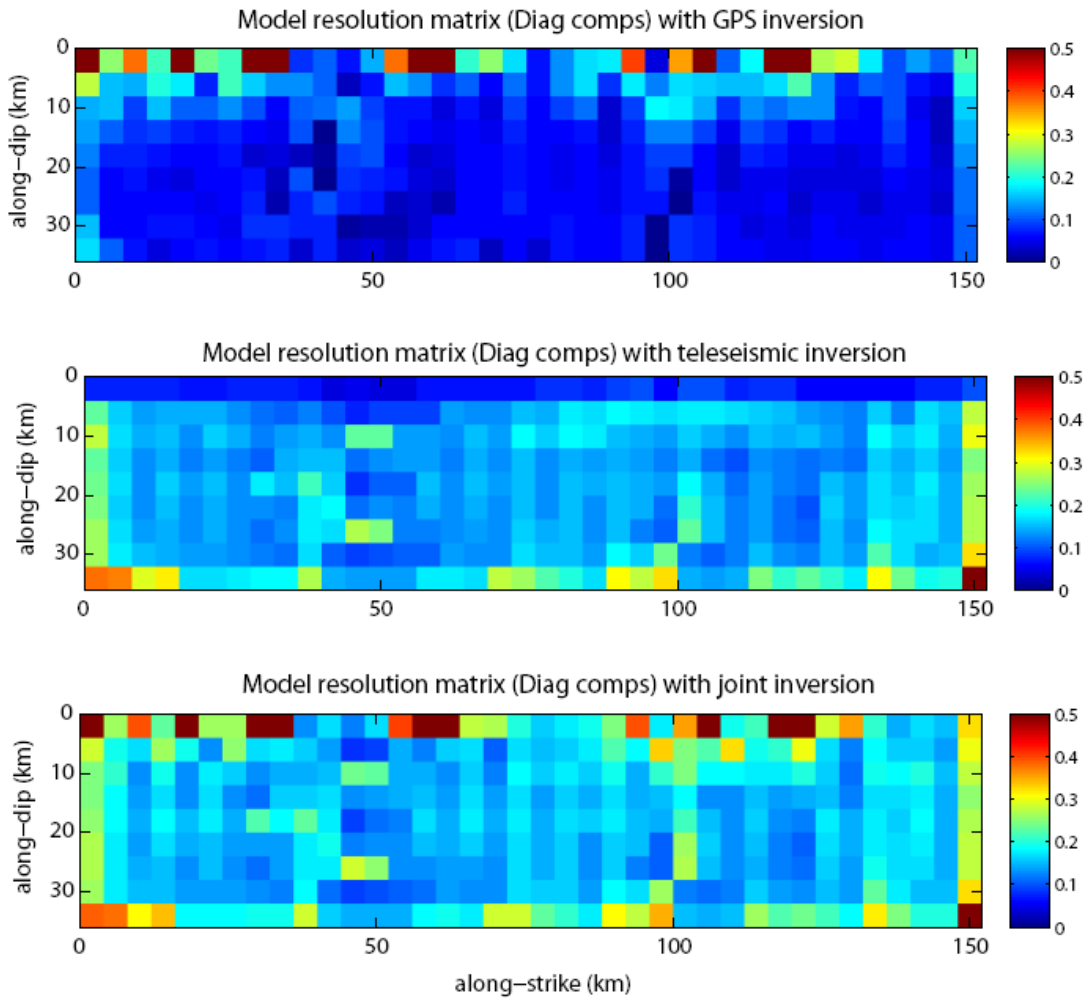


Figure 9. Model resolution obtained by three different sets of data (top: GPS, center: teleseismic, bottom: combined).

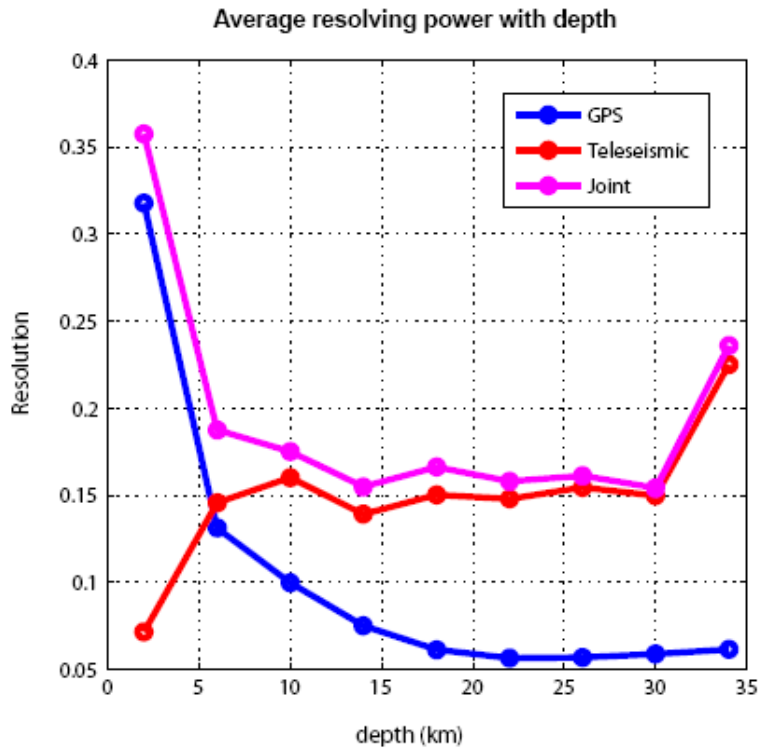


Figure 10. Average resolution as a function of depth.

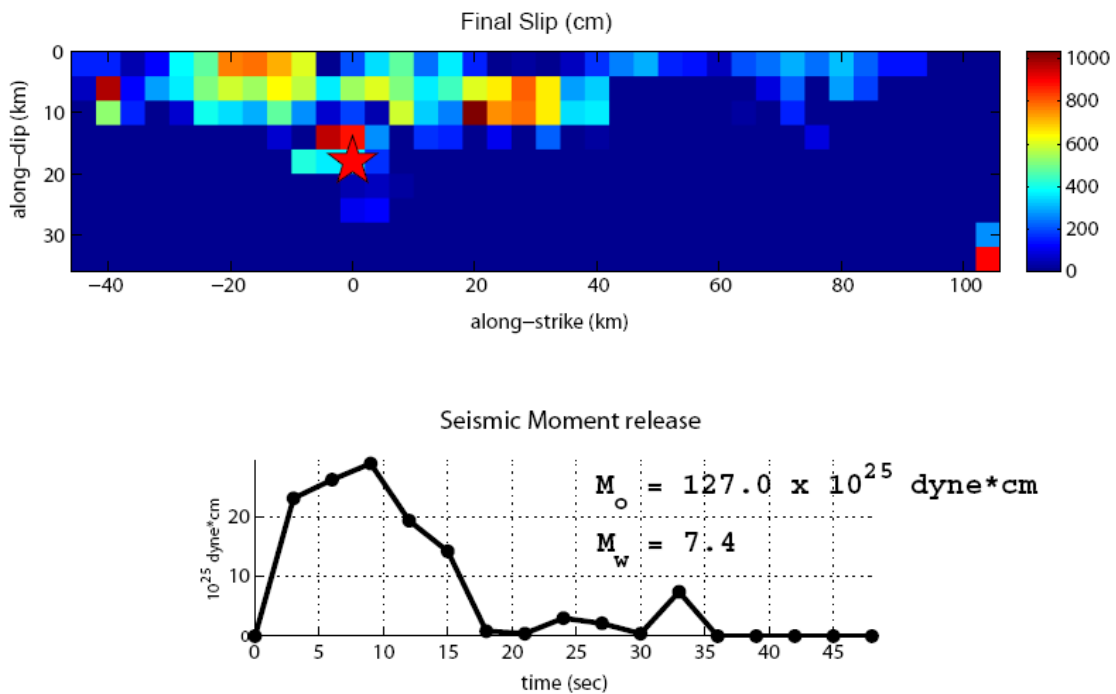


Figure 11. Final slip distribution and seismic moment release for the joint inversion. Figure 11 shows final slip distribution obtained by the joint inversion. Most deep slip (below 20 km)

observed in the geodetic inversion (see the bottom panel of Figure 6) is removed and the coseismic slip is extended down to about 20 km from the surface. Figures 12-14 show the teleseismic station locations and waveform comparisons for this inversion. We found that model resolution at depth can be improved by including seismic data in the inversion compared to inverting geodetic data alone, but still inversion results are strongly affected by non-physical regularization schemes (e.g., minimum norm, first or second order smoothing) used to reduce the instability of the inversion. Adjusting the level of smoothing, the depth extent of coseismic slip estimates for the event can be varied between 15 km and 25 km without reducing data fitting significantly although we invert both geodetic and seismic data jointly. Most estimates of the depth extent for the event obtained by various research groups are placed within this range (Yagi and Kikuchi, 2000; Bouchon et al., 2002; Delouis et al., 2002; Sekiguchi and Iwata, 2002). There may be several different factors to make the accurate estimate of the coseismic depth extent difficult, such as insufficient band-limited data, incorrect fault parameterization (e.g., fault geometry and grid spacing), incorrect Green's function, etc., but non-physical Tikhonov regularization (minimum norm, first or second order smoothing) is one of the main factors to contaminate the true depths of coseismic slip. In the next section we suggest a new type of source inversion based on the Bayesian framework, in which we can replace the nonphysical regularization schemes with more physics-based ones. We think that this new approach may enable us to do more physics-based interpretation of inversion results.

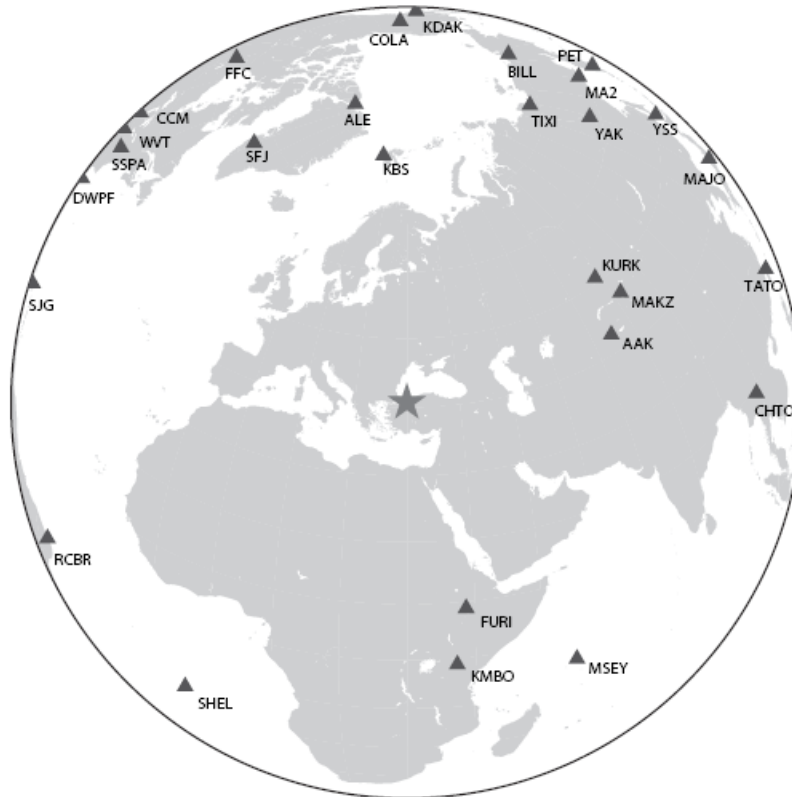


Figure 12. Teleseismic station locations for the Kocaeli, Turkey, event.

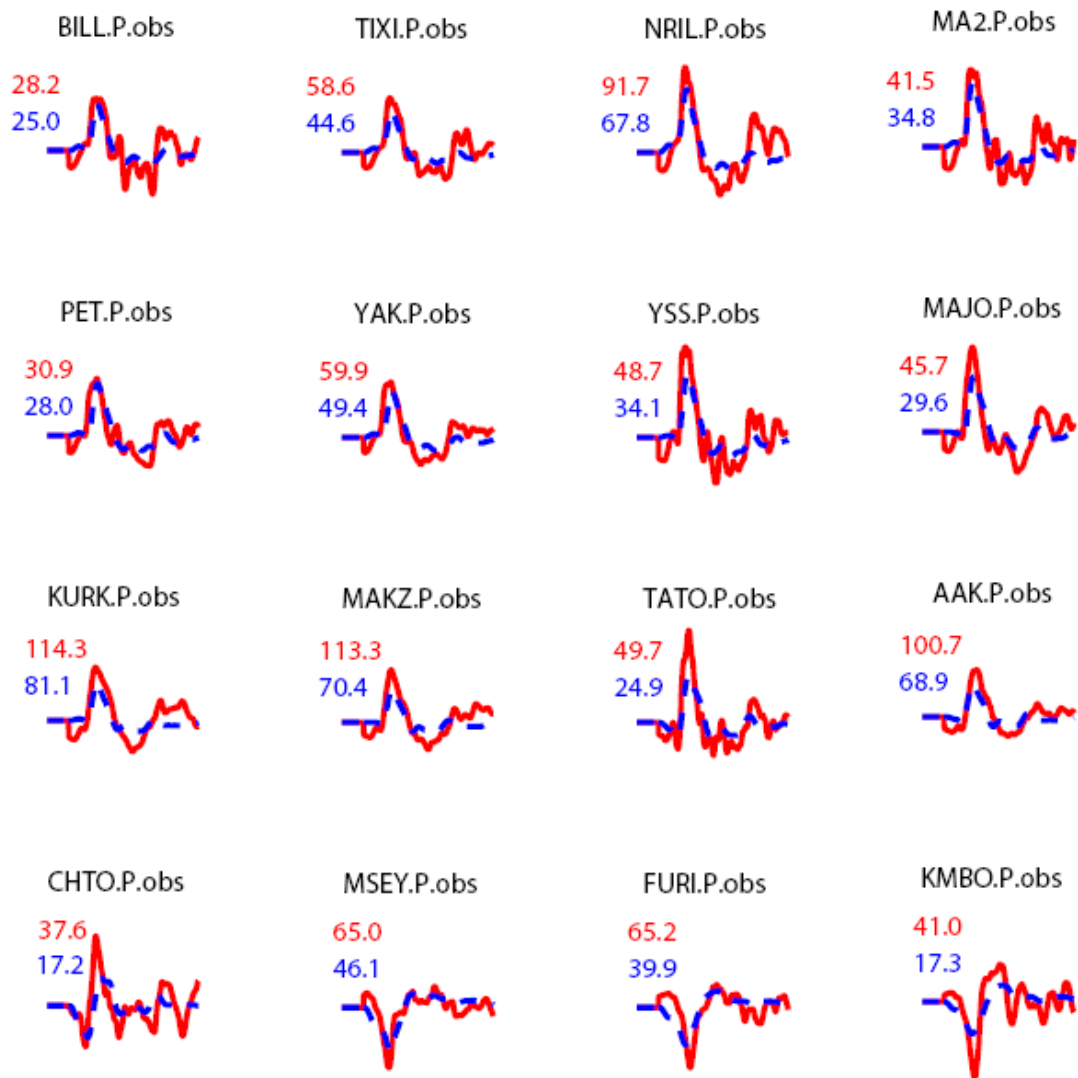


Figure 13. Telesismic waveform fitting.

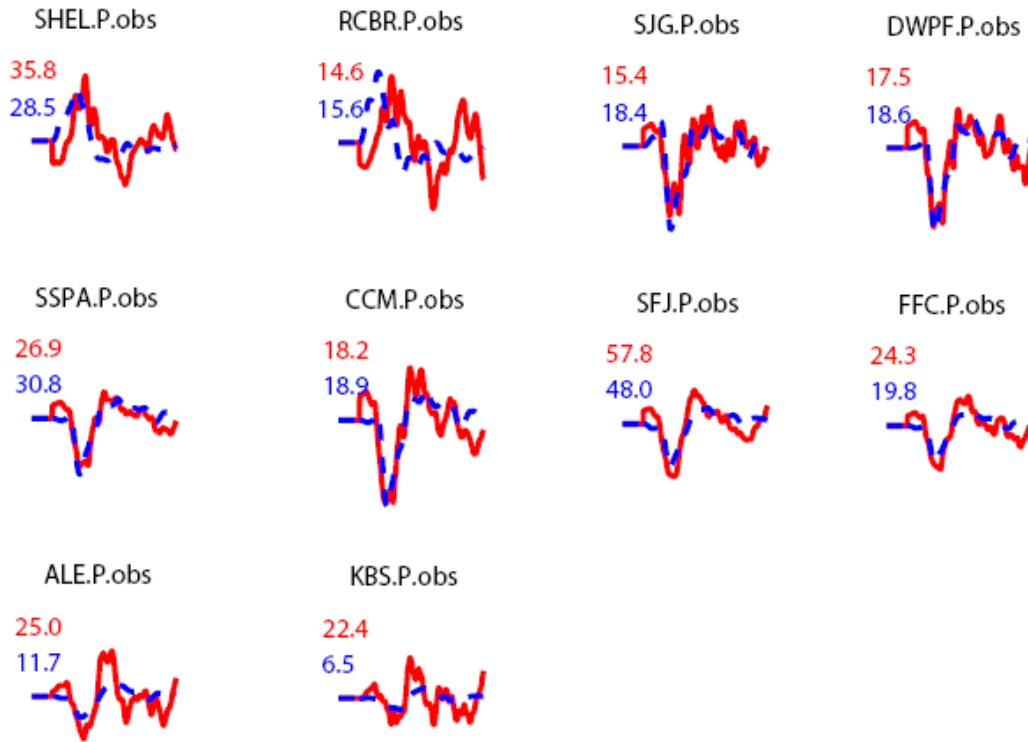


Figure 14. Teleseismic waveform fitting (continued).

4. Bayesian Inversion with Physically-guided Regularization

Most kinematic source inversion problems are very ill-posed because of insufficient data. Regularization (e.g., minimum norm or smoothing) is often used in order to reduce the instability of the inversion. If the degree of regularization is increased, the instability of the inversion is artificially reduced. The variance of model estimates is also reduced. This artificial regularization also reduces the resolving power of inversion estimators. In other words, there are trade-offs between the model resolution matrix and the model covariance matrix as we observed in section 2 above. This means that the regularization is helpful in reducing the instability of inverse problems, but at the same time it prevents accurate estimation of our model. The regularization also makes the estimators biased, which means that our solutions are not centered at the true solution. The bias of estimators makes accurate estimation of uncertainty difficult.

Several statistical measures are used to determine the appropriate level of regularization in a quantitative way, e.g., L-curve, cross-validation, and ABIC (Yoshida, 1989; Yabuki and Matsu'ura, 1992; Aster et al., 2005). Although these statistical measures may provide us with some optimal values for appropriate regularization, it is important to note that most regularization methods (e.g., minimum norm, first or second order smoothing) do not embody any physical bases. The estimated depth extent of coseismic slip is also significantly affected by non-physical regularization, which makes the physical interpretation of deep slip estimates difficult. In this section, we introduce a new type of inversion based on Bayesian inversion, in which the artificial regularization schemes are replaced with more physics-based ones, which enables us to do more physics-based interpretation of inversion results.

Bayesian inversion is becoming more and more popular in the geophysics community since high performance computing makes Monte Carlo simulation more feasible even in a high dimensional problem. The primary strength of Bayesian inversion that is well recognized by the geophysics community is that it produces distributions rather than a single point estimate. But the real advantage of the Bayesian inversion compared to classical approaches is that the prior distribution can be more rigorously used in the inversion procedure. There are two different perspectives on parameter estimation in statistics. Frequentists think that a single true solution exists, but it is unknown and it may be difficult to obtain the true solution, but we should solely rely on data and obtain our solution as objectively as possible. On the other hand, Bayesians think that true solutions can be described with probability density functions, i.e., the true solutions are random variables. And more importantly it is acceptable or even recommended to use our prior knowledge or information about the model in the inversion process.

Although it is desirable to invert both seismic and geodetic data, here we will illustrate a simple example of physically-guided regularization in finite earthquake source inversion with a set of GPS data inversion. If the multi-variate normal distribution is assumed in the prior distribution of the Bayesian inversion, the mean vector and covariance matrix completely define the prior distribution. The mean slip vector can be relatively easily obtained by available scaling laws between earthquake size (magnitude) and mean slip (Somerville et al., 1999). Since there is no scaling law available for the standard deviation of earthquake slip, it should be appropriately assumed in the inversion. The key innovation of this study is that we can use the off-diagonal components of the covariance matrix in the prior distribution to replace the classical non-physical regularization with more physics-based ones. If our model space is composed of slip distribution on a finite fault plane, the off-diagonal components of the covariance matrix are equivalent to the auto-correlation function or power spectral density of earthquake slip in the sense that they define the heterogeneity of slip distribution. We may be able to avoid arbitrary regularization by appropriately implementing the off-diagonal components of the covariance matrix in the inversion procedure.

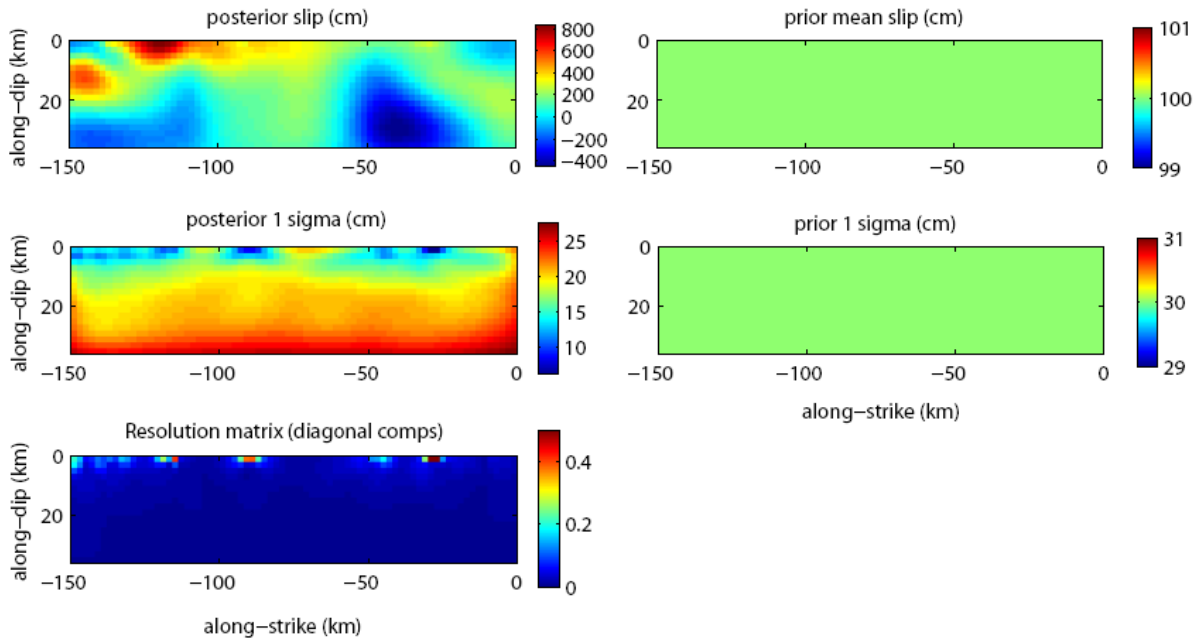


Figure 15. Prior and posterior mean slip distributions with their standard deviations, showing how the GPS data shape the slip distribution. The bottom panel shows the resolution of each subfault. If the subfaults are near the GPS stations, they have relatively high resolution, but the resolution in the geodetic inversion decays rapidly from the stations, especially with depth. The variance of the estimates is reduced

significantly in the high resolution subfaults.

We tested this idea with the same 1999 Izmit, Turkey, event with a set of GPS data. The right panel of Figure 15 shows the prior mean and sigma of earthquake slip and the left panel of Figure 15 shows the posterior mean and sigma of earthquake slip after the prior distribution is combined with the likelihood function, i.e., data-fitting function. The bottom panel on the left shows the diagonal components of the model resolution matrix that indicates that the resolving power of GPS data decay rapidly with depth. In this figure, we can see how the GPS data shaped our model from the prior in a space domain. In other words, we can update our model from the prior by analyzing available geophysical data. Figure 16 shows the auto-correlogram of earthquake slip for both the prior and posterior distribution. We used the auto-correlogram because it is the quantity that can be directly implemented in the covariance matrix (Song et al., 2009; Song and Somerville, 2009). It is equivalent to the auto-correlation function (ACF) or power spectral density (PSD) used in signal/image processing. Figure 16 shows that although we assume the exponential type decay of the auto-correlogram, the data prefers the Gaussian type decay in this case. The prior constraint used in this inversion can also be considered another type of regularization. But now we can argue whether the 1-point statistics (histogram) of earthquake slip follows Gaussian or non-Gaussian distribution and whether the data prefer faster or slower spectral decay of earthquake slip compared to prior constraints without using the classical Tikhonov type regularization.

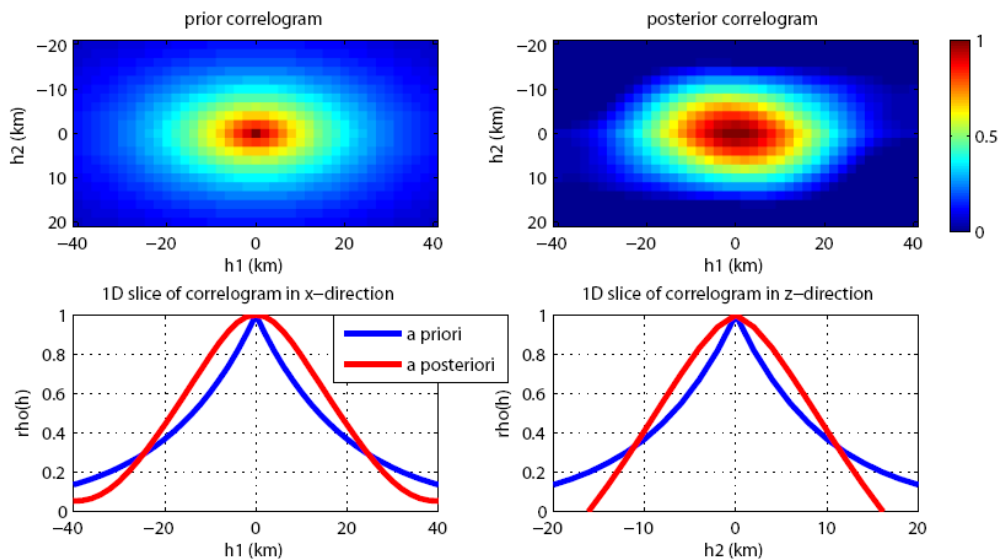


Figure 16. Prior and posterior auto-correlograms. The prior shows the exponential type decay while the posterior shows more Gaussian type decay.

Figure 17 (right panel) shows that we can set up our desired average slip distribution as a function of depth in the prior distribution and test how it is shaped by data in the inversion. Since geodetic data have very weak resolution for deep slip, we need to be careful in interpreting this inversion result, in particular with respect to the depth extent of coseismic slip. But we see the potential that this type of inversion approach enables us to do more physics-based regularization in the inversion, and consequently allow physics-based interpretation of inversion results.

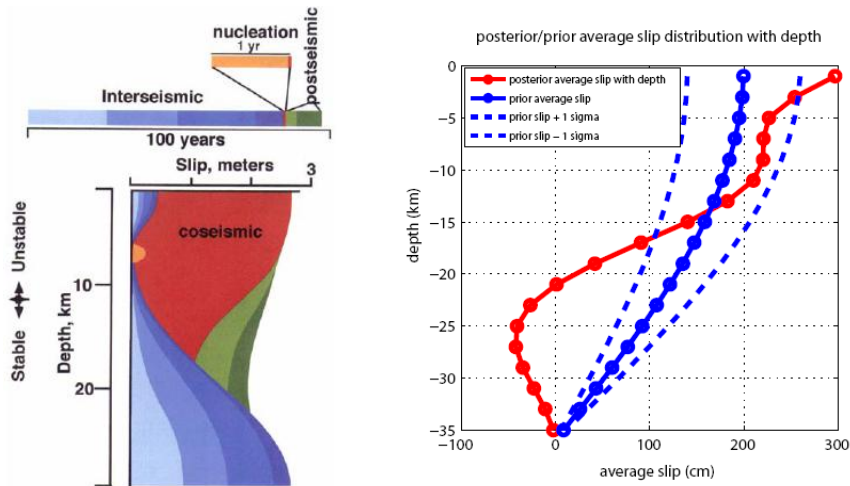


Figure 17. [left] Composition of slip as a function of depth (Scholz, 2002). [right] Prior and posterior average slip distribution with depth for the Kocaeli, Turkey, event.

5. Summary

We performed detailed analyses of model resolution in coseismic source inversion with both geodetic and seismic data in this study. We found that geodetic data alone do not have enough resolution to constrain slip at depth and joint inversion with seismic data is critical in improving resolution, in particular, at depth. We also suggested a new type of inversion method, in which we can avoid non-physical regularization (smoothing) that contaminates true solutions, or the true depth of coseismic slip, and replace it with more physically guided regularization in the Bayesian framework. This may enable us to resolve deep slip, avoiding the effect of the artificial smoothing.

Shaw and Wesnousky (2008) state in their paper that the key question regarding the depth of faulting is whether we can prove deep slip below the seismogenic zone from the observational point of view since some theoretical models clearly allow for the deep slip below the seismogenic zone and slip-length observations are nicely explained if deep slip occurs. In this study, we found that it is difficult to prove or disprove deep slip with currently available kinematic source inversion methods although we invert geodetic and seismic data jointly. A new inversion method, suggested in this report as ‘Bayesian inversion with physically-guided regularization,’ may enable us to resolve the deep slip in a more physics-based way in kinematic source inversion if multiple data sets are appropriately implemented, although we illustrate the new method only with geodetic data in this study.

6. References

- Aster, R.C., C.H. Thurber, and B. Borchers (2005). Parameter estimation and inverse problems, Elsevier Academic Press.
- Bouchon, M., M. Nafi Toksoz, H. Karabulut, M. Bouin, M. Dietrich, M. Aktar, and M. Edie, Space and time evolution of rupture and faulting during the 1999 Izmit (Turkey) earthquake, *Bull. Seism. Soc. Am.* **92**, 256-266.
- Delouis, B., D. Giardini, P. Lundgren, and J. Salichon (2002). Joint inversion of InSAR, GPS, Teleseismic, and strong-motion data for the spatial and temporal distribution of earthquake slip: application to the 1999 Izmit mainshock, *Bull. Seism. Soc. Am.* **92**, 278-299.

- Dieterich, J.H. (1972). Time dependent friction in rocks. *Journal of Geophysical Research* 77, 3690-3697.
- Ellsworth, W. (2006). Forecasting Magnitude from Fault Geometry. Proceedings of the 1 November 2006 Magnitude-Area relation summit convened by the Working Group for California Earthquake Probabilities. <http://gravity.usc.edu/WGCEP/activities/meetings/110106/index.html>.
- King, G.C.P. and S. Wesnousky (2007). Scaling of earthquake fault parameters. *Bull. Seism. Soc. Am.* **97**, 1833-1840.
- Mikumo, T. (1992). Dynamic fault rupture and stress recovery processes in continental crust under depth-dependent shear strength and frictional parameters. *Tectonophysics* 211, 201-222.
- Nazareth, J. and E. Hauksson (2004). The seismogenic thickness of the Southern California crust. *Bull. Seism. Soc. Am.* **94**, 940-960.
- Oglesby, D.D., D.S. Dreger, R.A. Harris, N. Ratchkovski, and R. Hansen (2004). Inverse kinematic and forward dynamic models of the 2002 Denali, Alaska earthquake. *Bull. Seism. Soc. Am.* **94**, S214-S233.
- Reilinger, R., S. Ergintav, R. Burgmann, S. McCluskey, O. Lenk, A. Barka, O. Gurkan, E. Hearn, K. L. Feigl, R. Cakmak, B. Aktug, H. Ozener, and M. N Toksoz (2000). Coseismic and postseismic fault slip for the 17 August 1999, M = 7.5, Izmit, Turkey earthquake, *Science* **289**, 1519-1524.
- Scholz, C.H. et al. (1972). Detailed studies of frictional sliding in granite and implications for the earthquake mechanism. *Journal of Geophysical Research* 77, 6392-6406.
- Scholz, C.H. (2002). The mechanics of earthquakes and faulting. Cambridge University Press, 2nd Edition.
- Sekiguchi, H., and T. Iwata (2002). Rupture process of the 1999 Kocaeli, Turkey, earthquake estimated from strong-motion waveforms, *Bull. Seism. Soc. Am.* **92**, 300-311.
- Shaw, B. E., and S. G. Wesnousky (2008). Slip-length scaling in large earthquakes: the role of deep-penetrating slip below the seismogenic layer, *Bull. Seism. Soc. Am.* **98**, 1633-1641.
- Somerville, P., K. Irikura, R. Graves, S. Sawada, D. Wald, N. Abrahamson, Y. Iwasaki, T. Kagawa, N. Smith, and A. Kowada (1999). Characterizing crustal earthquake slip model for the prediction of strong ground motion, *Seismol. Res. Lett.* **70**, 59-80.
- Somerville, P.G. and A. Pitarka (2006). Differences in earthquake source and ground motion characteristics between surface and buried earthquakes. *Proceedings of the Eighth National Conference on Earthquake Engineering*, San Francisco, California.
- Song, S., A. Pitarka, and P. Somerville (2009). Exploring spatial coherence between earthquake source parameters, *Bull. Seism. Soc. Am.* **99**, 2,564-2,571.
- Song, S., and P. Somerville (2009). Physics-based earthquake source modeling with Geostatistics, *Bull. Seism. Soc. Am.* in press.
- Stein, R. (2006). Report and recommendations of the 1 November 2006 Magnitude-Area relation summit convened by the Working Group for California Earthquake Probabilities. <http://gravity.usc.edu/WGCEP/activities/meetings/110106/index.html>.
- Thio, H.K. (2005). The rupture process of the 2002 Alaska earthquake. *Geophys. Res. Abstracts* **5**, 13753, European Geophysical Society.
- Thio, H. K., R. W. Graves, P. G. Somerville, T. Sato, and T. Ishii (2004). A multiple time window rupture model for the 1999 Chi-Chi earthquake from a combined inversion of teleseismic, surface wave, strong motion, and GPS data, *J. Geophys. Res.*, **109**, B08309, doi:10.1029/2002JB002381.
- Working Group on Earthquake Probabilities (2003). Earthquake probabilities in the San Francisco Bay Region: 2002 to 2031: A Summary of Findings. USGS OFR 03-214.
- Yabuki, T., and M. Matsu'ra (1992). Geodetic data inversion using a Bayesian information criterion for spatial distribution of fault slip, *Geophys. J. Int.* **109**, 363-375.
- Yagi, Y., and M. Kikuchi (2000). Source rupture process of the Kocaeli, Turkey, earthquake of August 17, 1999, obtained by joint inversion of near-field data and teleseismic data, *Geophys. Res. Lett.* **27**, 1969-1972.
- Yoshida, S. (1989). Waveform inversion using ABIC for the rupture process of the 1983 Hindu Kush earthquake, *Phys. Earth Planet. Inter.*, **56**, 389-405.